

# Cohesive zone modeling of cracking along the Cu/Si interface in nanoscale components

\*Y.B. Yan<sup>1</sup>, T. Sumigawa<sup>2</sup>, and T. Kitamura<sup>2</sup>

<sup>1</sup>Institute of Systems Engineering, China Academy of Engineering Physics, Miayang 621900, China.

<sup>2</sup>Department of Mechanical Engineering and Science, Kyoto University, Kyoto 606-8501, Japan.

\*Corresponding author: yanyabin@gmail.com

## Abstract

In this study, crack initiation and propagation along the Cu/Si interface in multilayered films (Si/Cu/SiN) with different thicknesses of the Cu layer (20 and 200 nm) are experimentally investigated using a nano-cantilever and millimeter-sized four-point bending specimens. To examine the cohesive zone model (CZM) criterion for interfacial delamination along the Cu/Si interface in nanoscale stress concentration, an exponential type of CZM is utilized to simulate the observed delamination processes using the finite element method. After the CZM parameters for the Cu/Si interface are calibrated by an experiment, interface cracking in other experiments is predicted. This indicates that the CZM criterion is universally applicable for describing cracking along the interface regardless of specimen dimensions and film thickness which include the differences in plastic behavior and residual stress. The CZM criterion can also predict interfacial cracking along Cu/Si interfaces with different stress singularities.

**Keywords:** Interface, Cohesive zone model, Delamination, Nanoscale, Thin films

## Introduction

Many micro-electronic and mechanical devices include bi-material interfaces, which, however, are liable to crack due to stress concentration originated from deformation mismatch [Rice (1998); Kitamura et al. (2002)]. So, for the assurance of reliability, it is important to evaluate the interface strength under nanoscale stress concentration.

Cohesive zone model (CZM) for cracking in bulk components has been successfully used for interfacial delamination in many material systems [Elices et al. (2002)]. However, the application for delamination induced by nanoscale stress concentration in small components has not been fully investigated. So, it is necessary to examine the applicability of CZM for fracture in nano-components. In this study, an exponential type of CZM is used to simulate the crack initiation at interface edge and propagation along the Cu/Si interface with nanoscale stress concentration in different experiments. The reliability of CZM concept for nano-components is examined on the basis of experiments and analyses.

## 1. Experiments on crack initiation and propagation

### 1.1 Tested materials

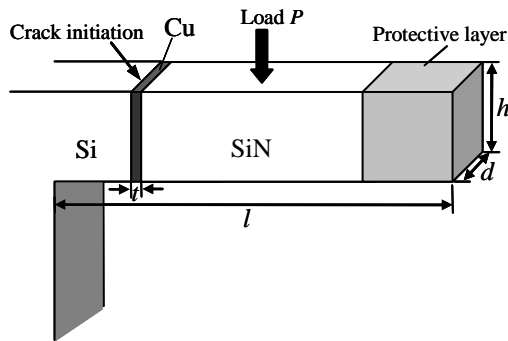
The tested materials are multilayer Si/Cu/SiN (silicon /copper/silicon nitride) with different Cu thicknesses. After a Si (100) wafer surface is cleaned by inverse sputtering, a Cu layer with a thickness of 20 or 200 nm is deposited by radio-frequency (RF) magnetron sputtering. A SiN thin layer of about 500 nm thickness is then formed on the Cu layer.

Since the Cu layer shows elasto-plastic behavior during experiments, the corresponding plastic properties of 20 nm [Sumigawa et al. (2010a)] and 200 nm [Takahashi et al. (2007)] thick Cu layers determined in previous experiments are used in following numerical calculations.

## 1.2 Specimens and experiment set-ups

### 1.2.1 Nano-cantilever experiment

Fig. 1 shows the specimen used for the nano-cantilever experiments of the Cu thin films of 20 and 200 nm thick (denoted as nano-cantilever (20 nm Cu) [Sumigawa et al. (2010b)] and nano-cantilever (200 nm Cu) [Hirakata et al. (2007)]). Crack initiation at interface edge is investigated here. A minute mechanical loading apparatus is used to apply a force and the behavior of interface fracture is observed in situ by transmission electron microscopy (TEM). The load is applied to the SiN layer with a diamond loading tip to apply stress to Cu/Si interface by a bending moment as shown in Fig. 1. No damage or defect is observed near the Cu/Si interface edge before the experiments.

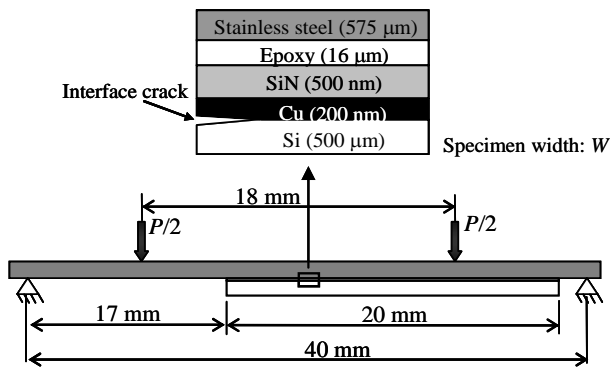


No.	$t$	$l$	$d$	$h$
A1		955	250	434
A2	20	840	308	233
A3		871	415	642
I1		1270	340	300
I2	200	1295	260	320
I3		1260	390	290
I4		762	320	980

**Fig. 1 Schematic illustration of nano-cantilever (20 nm Cu) and nano-cantilever (200 nm Cu) specimens (length unit: nm)**

### 1.2.2 Modified four-point bend experiment [Hirakata et al. (2007)]

A rectangular coupon with millimeter-scale width cut from the material with the 200 nm-thick Cu thin film is glued to a plate of stainless steel, as shown in Fig. 2. After a pre-crack is introduced, the load  $P$  is applied at a constant displacement rate. The whole specimen size is millimeter-scale, which is almost a thousand times larger than those of the nano-cantilever specimens. The study focus is the crack propagation along the Cu/Si interface from the pre-crack.



Specimen No.	$W$ , mm
P1	5.58
P2	4.79
P3	4.54

**Fig. 2 Schematic illustration of the modified four-point bend specimen (200 nm Cu) and the loading system**

## 1.3 Experimental results

### 1.3.1 Nano-cantilever experimental results

Fig. 3 shows the relationships between the applied load and deflection at the end of the cantilever arm under monotonic loading. With increasing the applied load, the experimental curves become nonlinear by plastic deformation of Cu layer. At the critical load, the crack initiates at interface edge

and immediately leads to the complete delamination of the entire interface. Similar fracture behavior is observed in the nano-cantilever (20 nm Cu) experiments. The critical loads,  $P_C$ , for crack initiation are listed in the table of Fig. 3, which shows great dependency on specimen geometry.

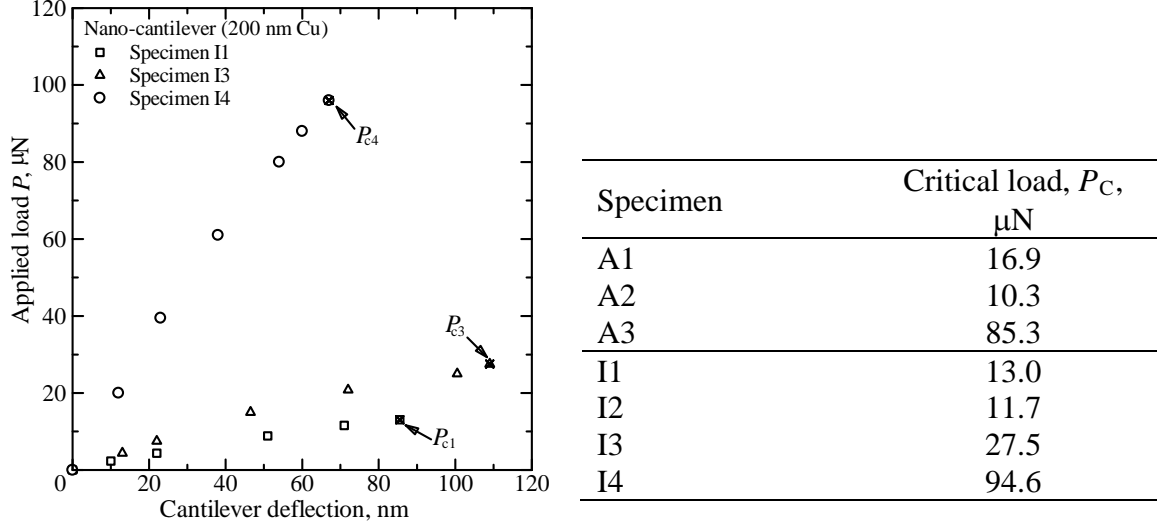


**Fig. 3 Relationship between applied load and cantilever deflection for specimens I1, I3, and I4, and the critical loads of all tested nano-cantilever specimens**

### 1.3.2 Modified four-point bend experimental results

Table 1 shows critical loads,  $P_C$ , for crack propagation in all the tested specimens. The obtained critical loads are nearly a million times larger than those in the nano-cantilever tests due to the huge difference in specimen dimensions.

**Table 1 Critical loads of four-point bend (200 nm Cu) specimens**

Specimen No.	Critical load $P_C$ , $\mu\text{N}$
P1	$5.40 \times 10^6$
P2	$4.86 \times 10^6$
P3	$4.65 \times 10^6$

## 2. Cohesive zone model

In the exponential CZM [Xu and Needleman (1993)], with increasing interfacial separation, the tractions across the interface increase to reach a maximum, and then decrease, eventually vanishing with complete decohesion.

The interfacial potential is defined as

$$\phi(\Delta_n, \Delta_t) = \phi_n + \phi_n \exp\left(-\frac{\Delta_n}{\delta_n}\right) \left\{ \left[1 - r + \frac{\Delta_n}{\delta_n}\right] \frac{1-q}{r-1} - \left[ q + \left(\frac{r-q}{r-1}\right) \frac{\Delta_n}{\delta_n} \right] \exp\left(-\frac{\Delta_t}{\delta_t}\right) \right\} \quad (1)$$

where  $\Delta_t = \sqrt{\Delta_{t1}^2 + \Delta_{t2}^2}$ ,  $q = \phi_t / \phi_n$ , and  $r = \Delta_n^* / \delta_n$ .  $\phi_n$  and  $\phi_t$  are the work of the normal and shear separations;  $\Delta_n$  and  $\Delta_t$  are the normal and shear displacement jumps, respectively;  $\delta_n$  and  $\delta_t$  are the normal and shear interface characteristic length parameters, respectively.  $\Delta_n^*$  is the critical magnitude of  $\Delta_n$  at complete shear separation, where normal traction is zero.

The relations between the interfacial tractions and the potential are given by

$$T_n = \frac{\partial \phi}{\partial \Delta_n}, \text{ and } T_t = \frac{\partial \phi}{\partial \Delta_t}. \quad (2)$$

Substituting Eq. (1) into Eq. (2), we obtain the interfacial tractions as follows

$$T_n = \left(\frac{\phi_n}{\delta_n}\right) \exp\left(-\frac{\Delta_n}{\delta_n}\right) \left\{ \frac{\Delta_n}{\delta_n} \exp\left(-\frac{\Delta_t^2}{\delta_t^2}\right) + \frac{1-q}{r-1} \left[1 - \exp\left(-\frac{\Delta_t^2}{\delta_t^2}\right)\right] \left(r - \frac{\Delta_n}{\delta_n}\right) \right\} \quad (3)$$

$$T_t = \frac{\phi_n}{\delta_n} \left(\frac{2\delta_n}{\delta_t}\right) \frac{\Delta_t}{\delta_t} \left(q + \frac{r-q}{r-1} \frac{\Delta_n}{\delta_n}\right) \exp\left(-\frac{\Delta_n}{\delta_n}\right) \exp\left(-\frac{\Delta_t^2}{\delta_t^2}\right) \quad (4)$$

The normal and shear cohesive energy (works of normal and shear separations) are related to  $\sigma_{\max}$  and  $\tau_{\max}$  by

$$\phi_n = \sigma_{\max} \delta_n \exp(1), \quad \phi_t = \sqrt{\exp(1)/2} \tau_{\max} \delta_t \quad (5)$$

Fig. 4 shows the traction-separation relationships for (a) normal and (b) shear separation.

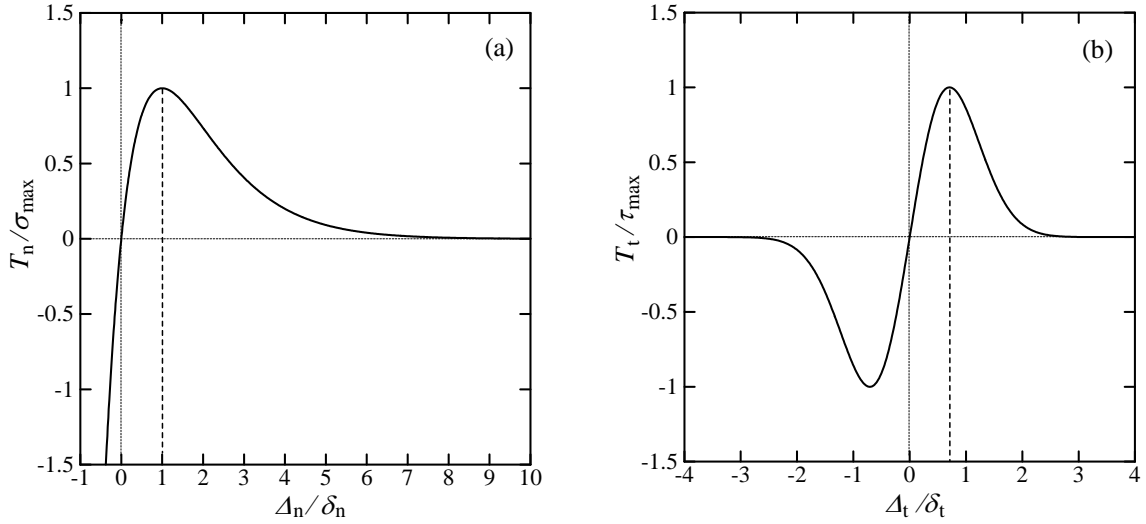


**Fig. 4 (a) Normal and (b) shear traction-separation curves for the exponential CZM**

### 3. Determination of CZM parameters

The CZM parameters are determined by calibrating the experimental results for specimen I1, which is one of the nano-cantilever (200 nm Cu) tests. Since the normal stress dominates the crack initiation and propagation in the nano-cantilever and four-point bend specimens, only the CZM parameters for normal separation need to be calibrated, *i.e.*  $\sigma_{\max}$  and  $\delta_n$ .

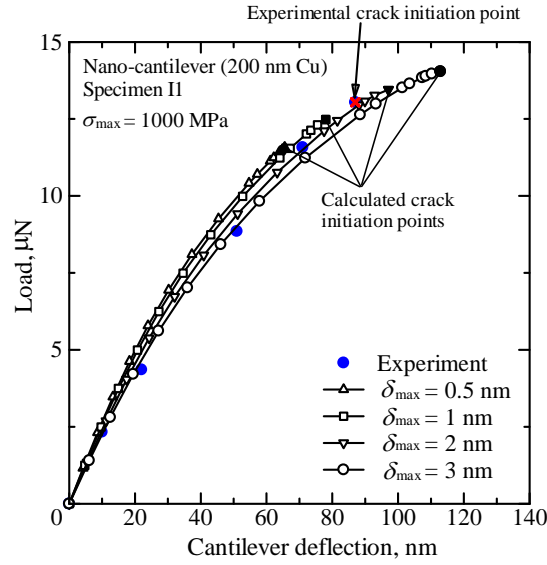


**Fig. 5 Effect of interface characteristic length parameter,  $\delta_n$ , on the calculated load-deflection curves**

With  $\sigma_{\max} = 1000$  MPa, the effect of the interface characteristic length parameter,  $\delta_n$ , is investigated using the experimental data of specimen II. As shown in Fig. 5, the slope of the calculated load-deflection curve is sensitive to the value of  $\delta_n$ . With decreasing  $\delta_n$ , the slope of the calculated curve becomes steep. The simulation for  $\delta_n = 1$  nm results in the best correspondence with the experimental data. Then,  $\delta_n = 1$  nm is used in subsequent calculations.

Fig. 6 shows the calculated load-deflection curves with different cohesive strengths under  $\delta_n = 1$  nm. The right figure gives an enlarged view of the square region in the left near the critical load. When the cohesive strength increases, the critical lateral forces become larger. The simulation with  $\sigma_{\max} = 1060$  MPa gives good prediction for the critical lateral force with the experimental results.

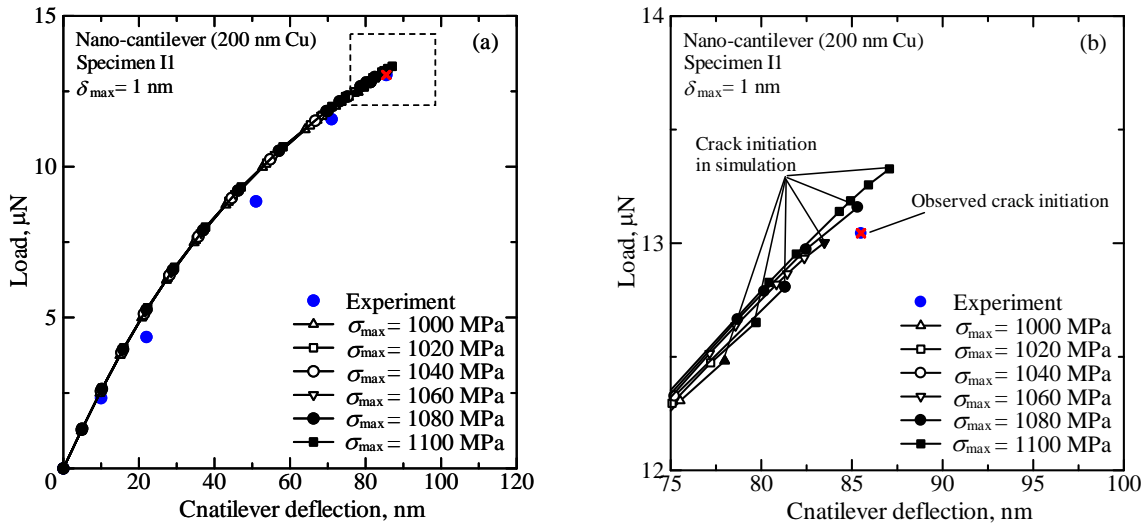


**Fig. 6 Effect of the cohesive strength,  $\sigma_{\max}$ , on the calculated critical loads for crack initiation**

From the calibration, the CZM parameters of the Cu/Si interface are determined to be  $\sigma_{\max} = 1060$  MPa, and  $\delta_n = 1$  nm, which give normal cohesive energy  $\phi_n = 2.85$  J/m<sup>2</sup>.

#### 4. Prediction of delamination with CZM parameters

All the experimental and predicted critical loads are compared in Fig. 7. Although the critical load magnitude has a difference of nearly 6 orders, the CZM parameters solely determined by specimen I1 can still universally predict interface cracking along Cu/Si interface cracking regardless of specimen dimensions and film thickness which include the differences in plastic behavior and residual stress. The good prediction both on the crack initiation at interface edge and propagation from a pre-crack tip indicates that the CZM criterion can describe cracking along Cu/Si interfaces with different stress singularities. These prove the versatility of the CZM criterion for the design of micro/nano devices.

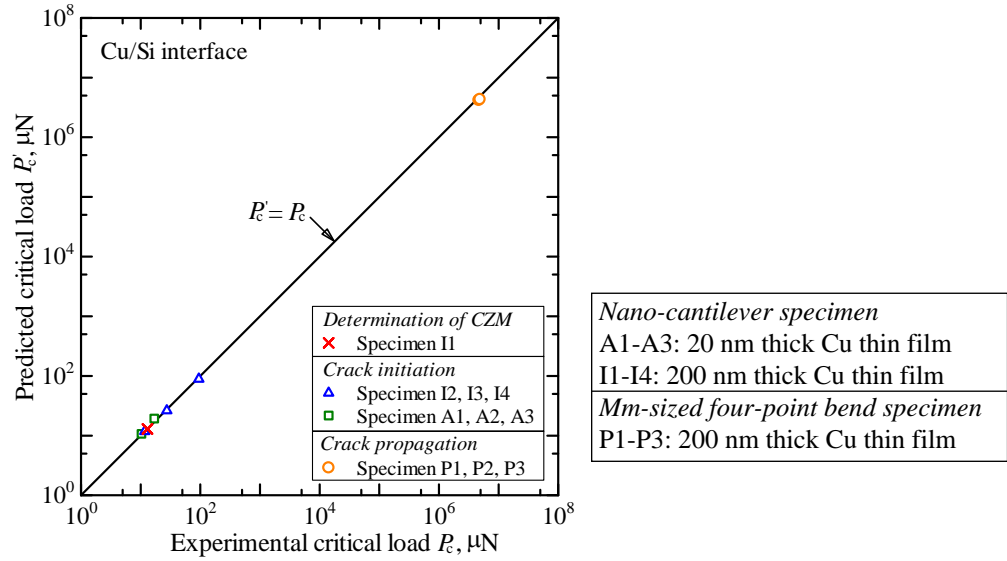


**Fig. 7 Comparison of experimental and predicted critical loads of all tested specimens**

#### 5. Conclusions

We have investigated the universal applicability of CZM to the initiation and the propagation of interface cracking in nano-cantilever (20 nm and 200 nm Cu) tests and modified four-point bending (200 nm Cu) tests. The results obtained can be summarized as follows:

- (1) By calibrating with the experimental results of the nano-cantilever (200 nm Cu) test, the CZM parameters of the Cu/Si interface were determined as follows: cohesive strength  $\sigma_{\max} = 1060$  MPa and interface characteristic length parameter  $\delta_n = 1$  nm.
- (2) The obtained CZM parameters give excellent prediction of crack initiation at the Cu/Si interface edge in nano-cantilever (20 nm Cu) and (200 nm Cu) experiments regardless of the specimen geometry, plastic behavior and residual stress.
- (3) The CZM predicts the crack propagation along the Cu/Si interface in the mm-sized modified four-point bending (200 nm Cu) specimen very well, though the specimen size has a difference of thousands of times. Moreover, this also shows the validity of the CZM parameters for prescribing the interface toughness under different stress singularities.

#### References

Elices, M., Guinea, G.V., Gomez, J., Planas, J. (2002) The cohesive zone model: advantages, limitations and challenges, *Engineering Fracture Mechanics*, **69**, 137–163.

- Hirakata, H., Takahashi, Y., Truong, D.V., Kitamura, T. (2007) Role of plasticity on interface crack initiation from a free edge and propagation in nano-component, *International Journal of Fracture*, **145**, 261–271.
- Kitamura, T., Shibutani, T., and Ueno, T. (2002) Crack initiation at free edge of interface between thin films in advanced LSI, *Engineering Fracture Mechanics*, **69**, 1289–1299.
- Rice, J.R. (1988) Elastic fracture mechanics concepts for interfacial cracks, *Journal of Applied Mechanics* **55**, 98–103.
- Sumigawa, T., Shishido, T., Murakami, T., Iwasaki, T., Kitamura T. (2010a) Evaluation on plastic deformation property of copper nano-film by nano-scale cantilever specimen, *Thin solid films*, **518**, 6040–6047.
- Sumigawa, T., Shishido, T., Murakami, T., Kitamura, T. (2010b) Interface crack initiation due to nano-scale stress concentration, *Materials Science and Engineering A*, **527**, 4796–4803.
- Takahashi, Y., Hirakata, H., Kitamura, T., (2007) Quantitative evaluation of plasticity of a ductile nano-component, *Thin Solid Films*, **516**, 1925–1930.
- Xu, X.P., and Needleman, A. (1993) Void nucleation by inclusion debonding in a crystal matrix, *Modelling and Simulation in Materials Science and Engineering*, **1**, 111–132.